SUPPLEMENTARY INFORMATION

Photochromism and Efficient Photothermal Conversion of B←N Lewis Adducts Induced by Intramolecular Electron Transfer

Sotaro Kusumoto,*[a] Takuma Mio,[a] Kenta Rakumitsu,[b] Masaya Shimabukuro,[c] Mamiko Kobayashi,[c] Tomoya Fukui,[d] Nobutsugu Hamamoto,[e] Toshiharu Ishizaki,[f] Yang Kim,[g] Yoshihiro Koide*[a]

[a] *Department of Applied Chemistry, Faculty of Chemistry and Biochemistry, Kanagawa University, 3-27-1 Rokkakubashi, Kanagawa-ku, Yokohama 221-8686, Japan.*
[b] *Graduate School of Pharmaceutical Sciences, Chiba University, 1-8-1 Inohana, Chuo-ku, Chiba 260-8675, Japan.*
[c] *Institute of Biomaterials and Bioengineering, Tokyo Medical and Dental University, 2-3-10, Kanda-Surugadai, Chiyoda-ku, Tokyo 101-0062, Japan.*
[d] *Laboratory for Chemistry and Life Science, Institute of Innovative Research, Tokyo Institute of Technology, 4259 Nagatsuta-cho, Midori-ku, Yokohama, Kanagawa 226-8501, Japan*
[e] *Research Center for Autonomous Systems Materialogy (ASMat), Institute of Innovative Research, Tokyo Institute of Technology, 4259 Nagatsuta-cho, Midori-ku, Yokohama, Kanagawa 226-8501, Japan.*
[f] *Department of Applied Chemistry, Faculty of Engineering, Sanyo-Onoda City University, Sanyo-Onoda, Yamaguchi 756-0884, Japan.*
[g] *Department of Chemistry, College of Humanities and Sciences, Nihon University, 3-25-40 Sakurajosui, Setagaya-ku, Tokyo 156-8550, Japan.*
[h] *Department of Chemistry, Graduate School of Science and Technology, Kumamoto University, 2-39-1 Kurokami, Chuo-ku, Kumamoto 860-8555, Japan.*

Corresponding author: S. Kusumoto, Y. Koide E-mail: kusumoto@kanagawa-u.ac.jp, ykoide01@kanagawa-u.ac.jp

Table S1. Crystallographic data of **1**-**4**.

Compound	**1**	**2**	**3**	**4**
formula	$C_{23}H_{21}BN_2$	$C_{24}H_{22}BN$	$C_{25}H_{24}BN$	$C_{24}H_{23}BN_2$
formula weight	336.23	335.23	349.26	350.25
crystal system	monoclinic	monoclinic	monoclinic	monoclinic
space group	$P\,2_1/c$	$P\,2_1/n$	$P\,2_1/c$	$P\,2_1/c$
a / Å	7.5903(3)	9.1472(13)	8.0933(4)	7.9199(7)
b / Å	15.2696(6)	21.758(2)	15.3063(7)	15.2320(14)
c / Å	16.0589(7)	9.8661(12)	16.4990(8)	16.2310(15)
α / º	90	90	90	90
β / º	92.043(4)	106.220(14)	96.802(5)	91.019(8)
γ / º	90	90	90	90
V / Å^3	1860.06(13)	1885.4(4)	2029.49(17)	1957.7(3)
Z	4	4	4	4
T / K	120	120	120	120
R_1	0.0763	0.0762	0.0605	0.0623
R_1 (all data)	0.1317	0.1828	0.1040	0.0980
wR_2	0.1967	0.1529	0.1379	0.1529
wR_2 (all data)	0.2617	0.2084	0.1621	0.1758
G.O.F.	1.050	1.044	1.039	1.045
CCDC	2379690	2379691	2379693	2379694

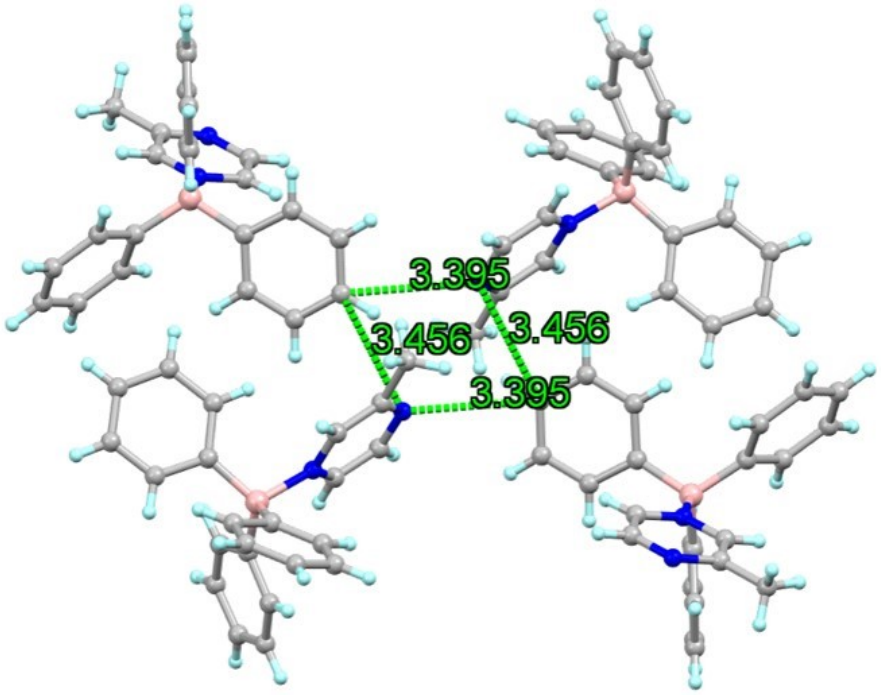

Figure S1 N· · · H hydrogen bonding in **1** (The distance is indicated between the C---N atoms.)

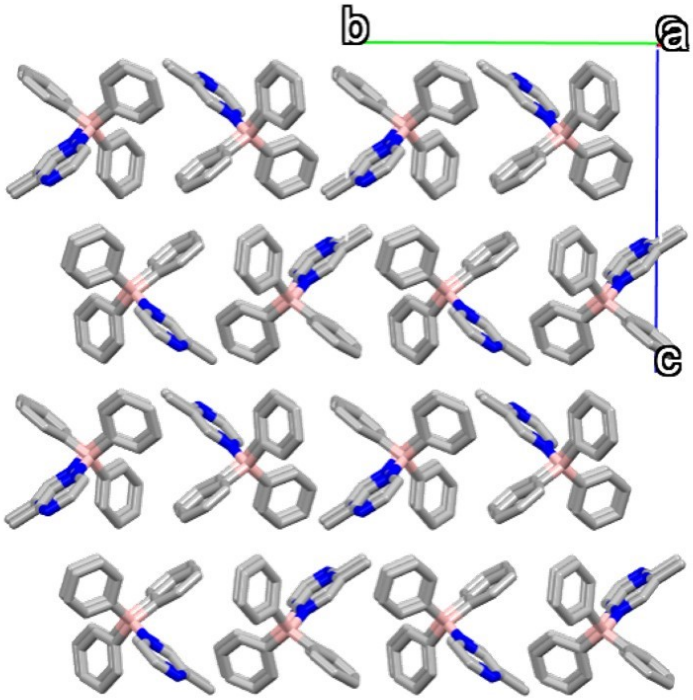

Figure S2 Packing structure of **1** viewed down *a*-axis.

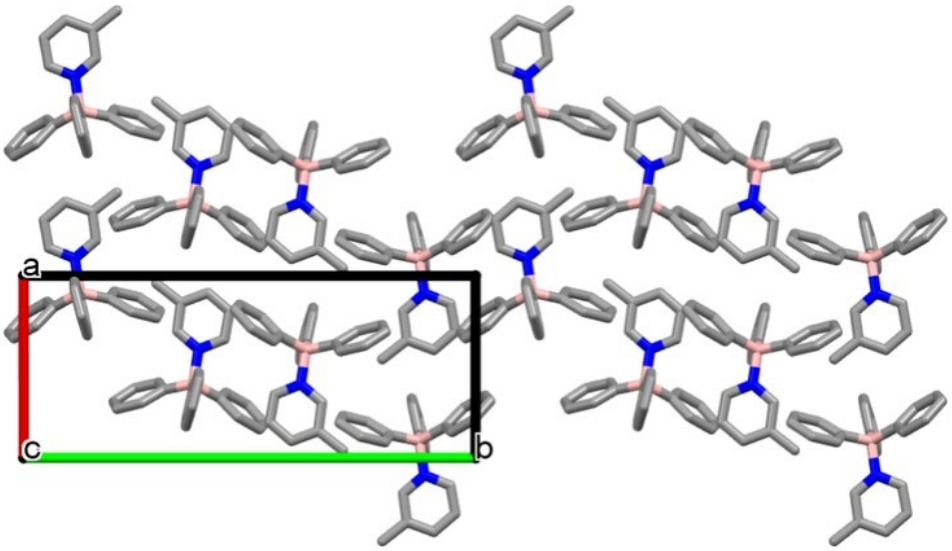

Figure S3 Packing structure of **2** viewed down *c*-axis.

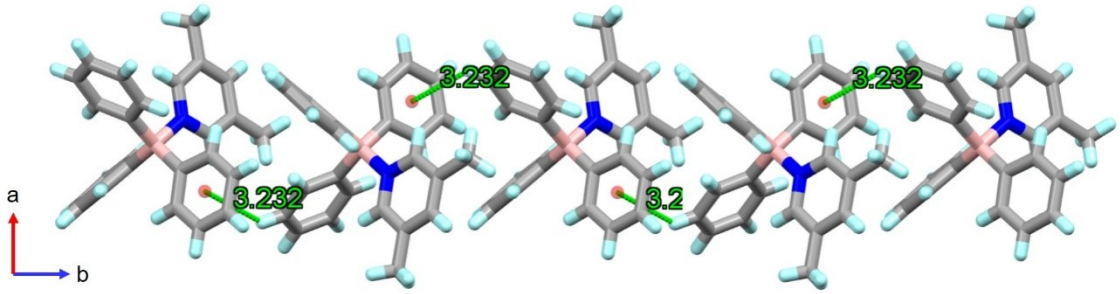

Figure S4 Intermolecular C-H· · · π interactions in **3**.

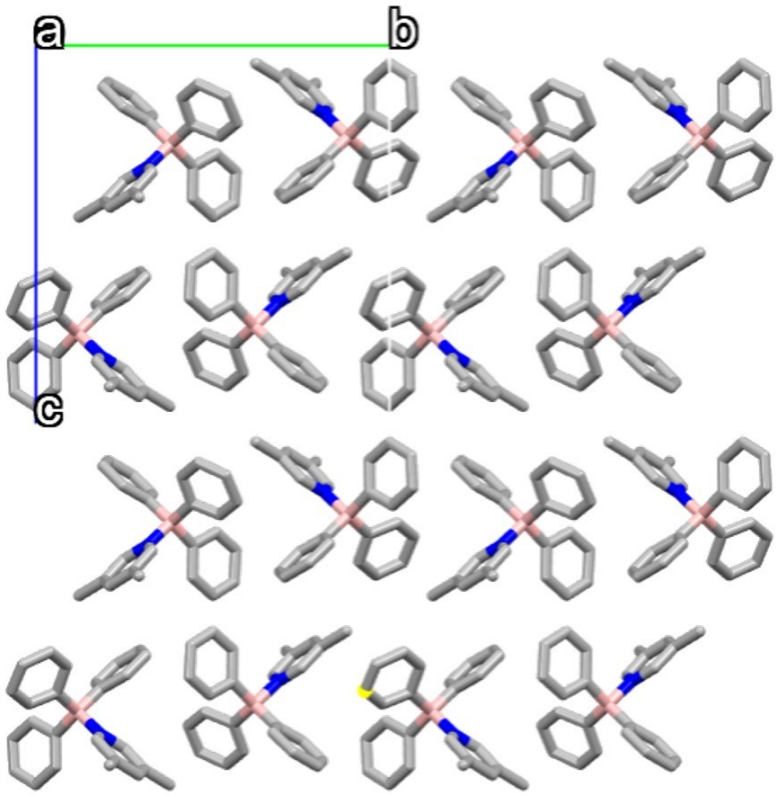

Figure S5 Packing structure of **3** viewed down *c*-axis.

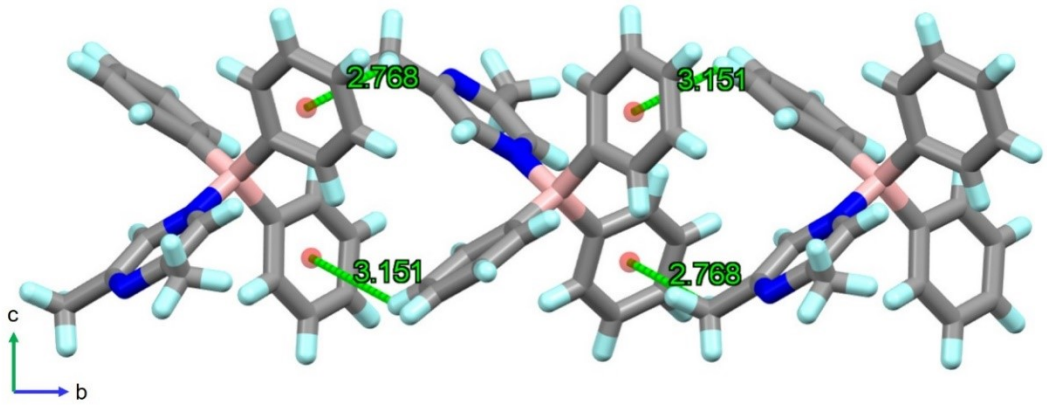

Figure S6 Intermolecular C-H· · · π interactions in **4**.

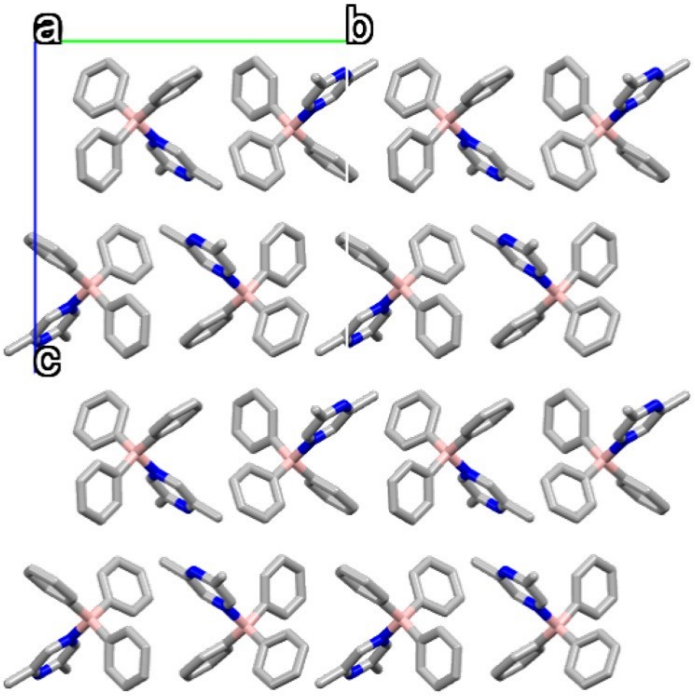

Figure S7 Packing structure of **4** viewed down *a*-axis.

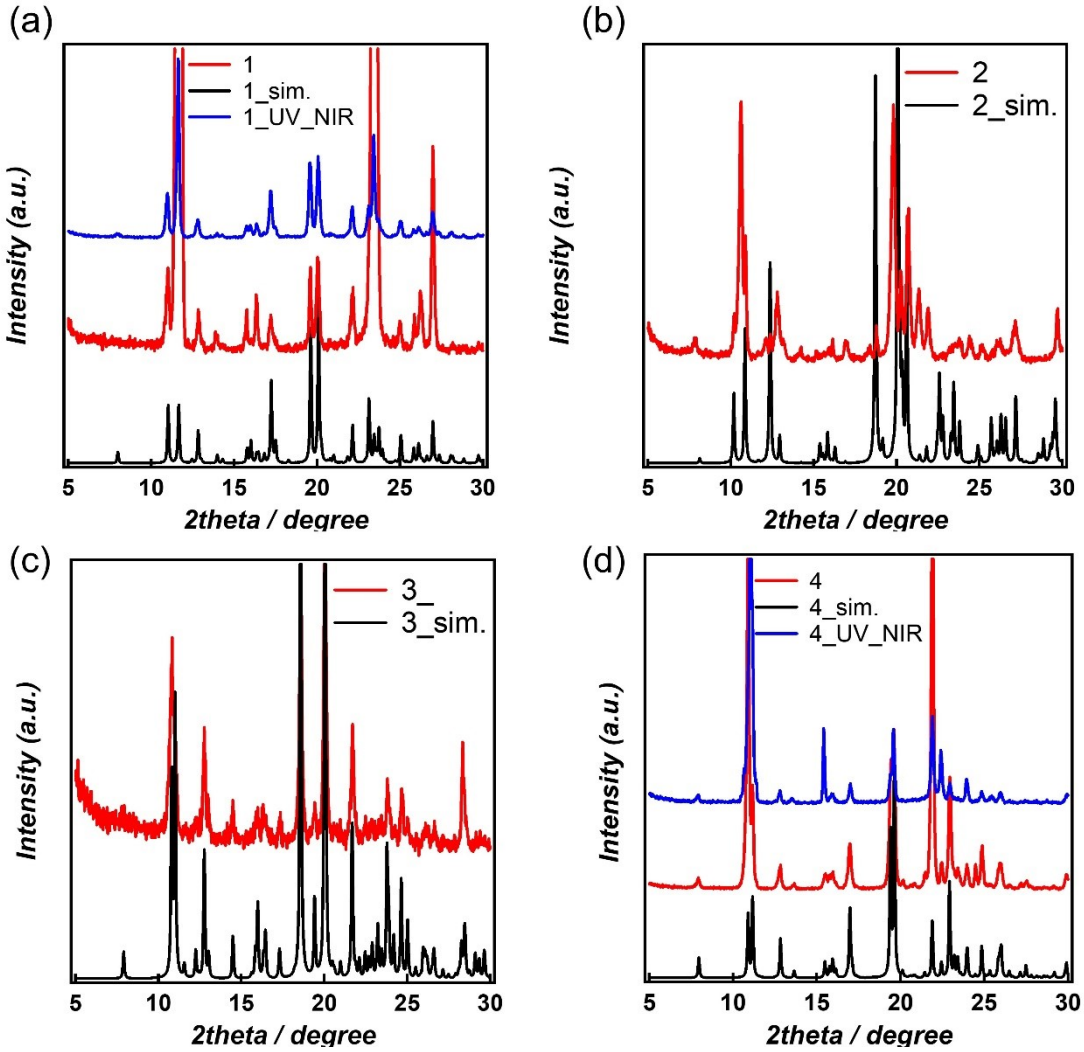

Figure S8 PXRD measurements for **1** (a), **2** (b), **3** (c), and **4** (d). **1**_sim, **2**_sim, **3**_sim, and **4**_sim are simulated XRD patterns, respectively. **1**_UV_NIR and **4**_UV_NIR represent PXRD patterns of compounds exposed to UV light (365 nm) and then to NIR light (850 nm) for 10 minutes.

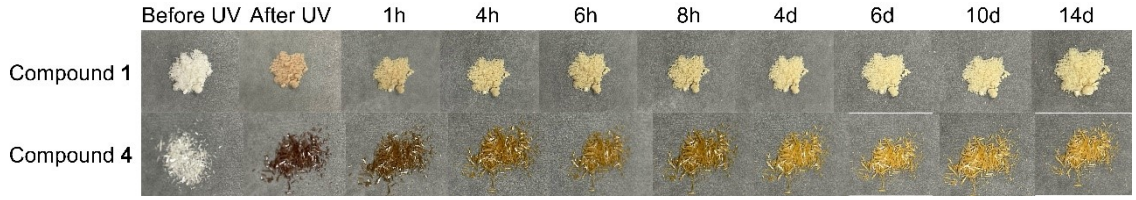

Figure S9 Photos of **1** and **4** before and after UV exposure. Photos that change color over time after turning off UV.

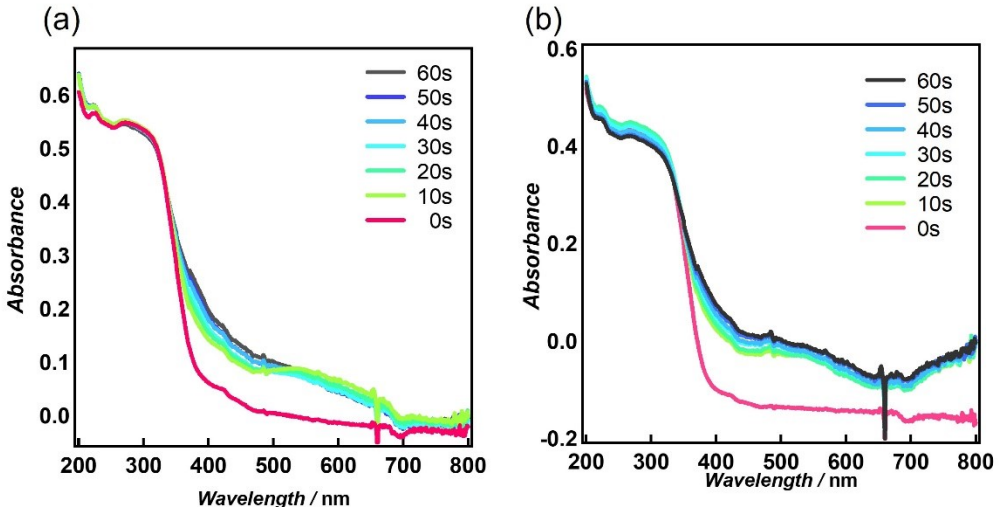

Figure S10 Time-dependent solid-state UV spectra of compounds **1** (a) and **4** (b) under UV irradiation.

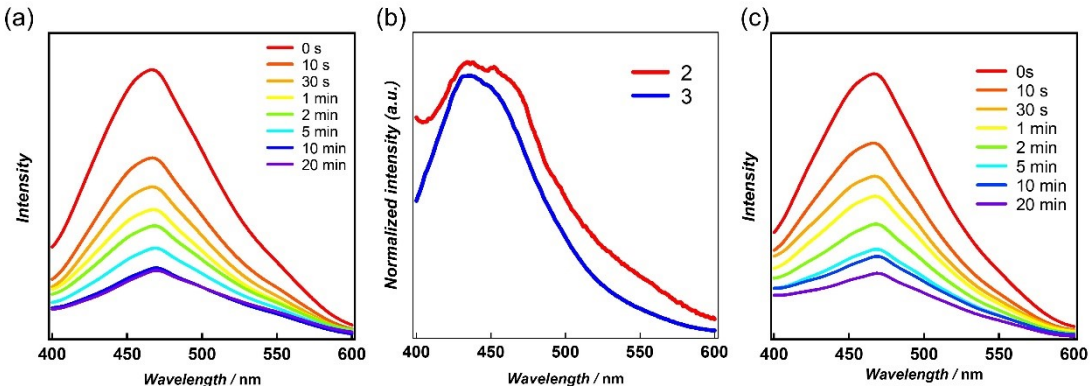

Figure S11 Time-dependent luminescence spectra by UV exposure of 1 (a) and 4 (c) and luminescence spectra of **2** and **3** (b).

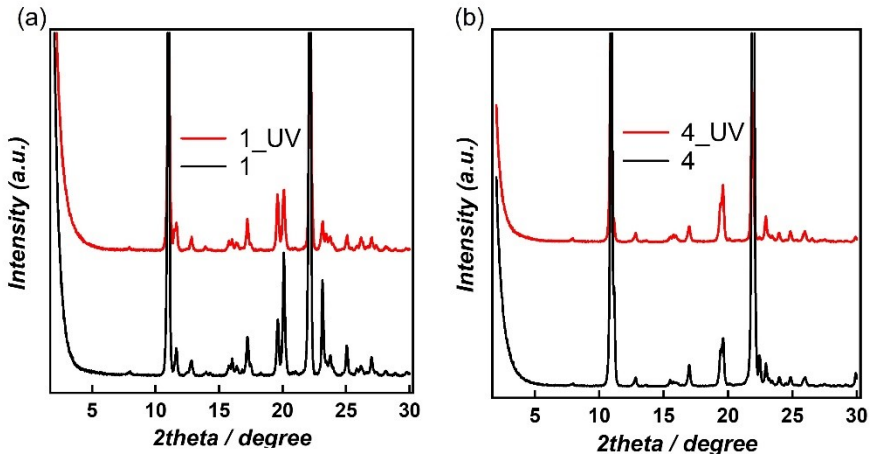

Figure S12 PXRD measurements of **1** (a) and **4** (b) conducted before and after UV irradiation.

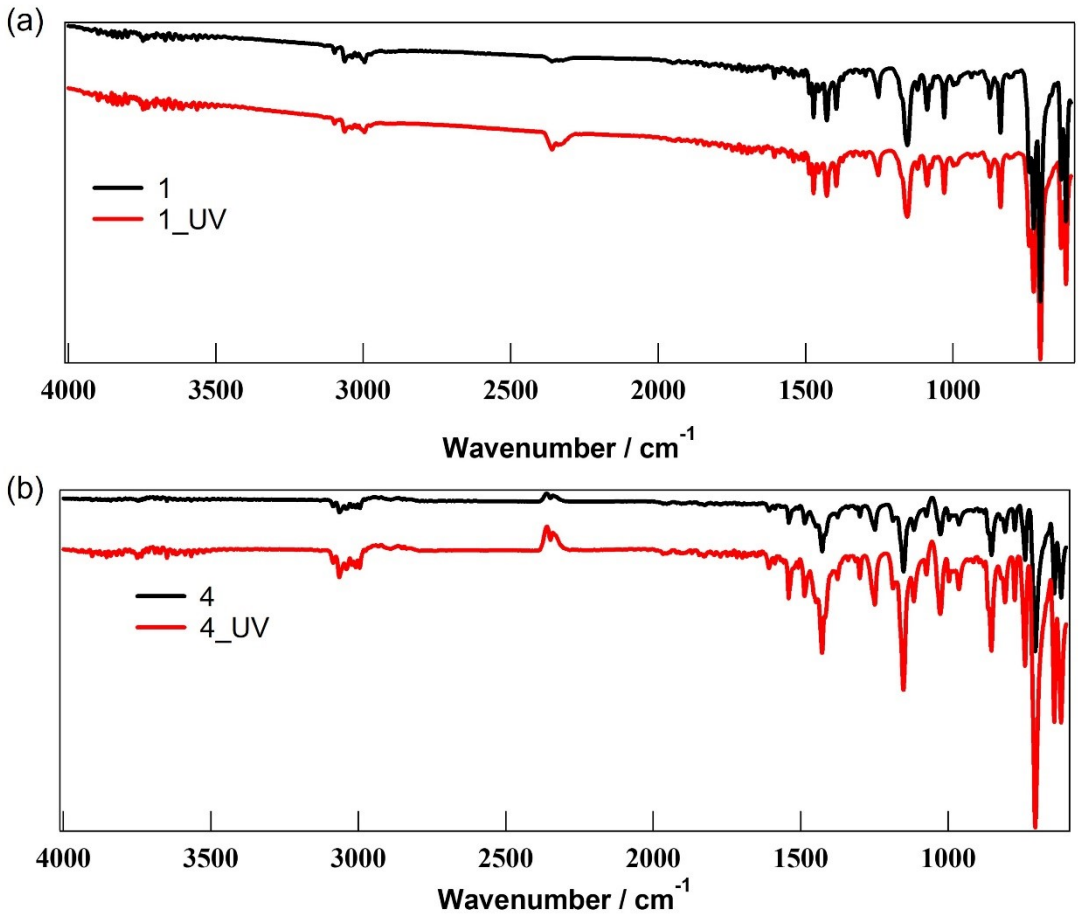

Figure S13 IR spectra of **1** (a) and **4** (b) measured before and after UV irradiation.

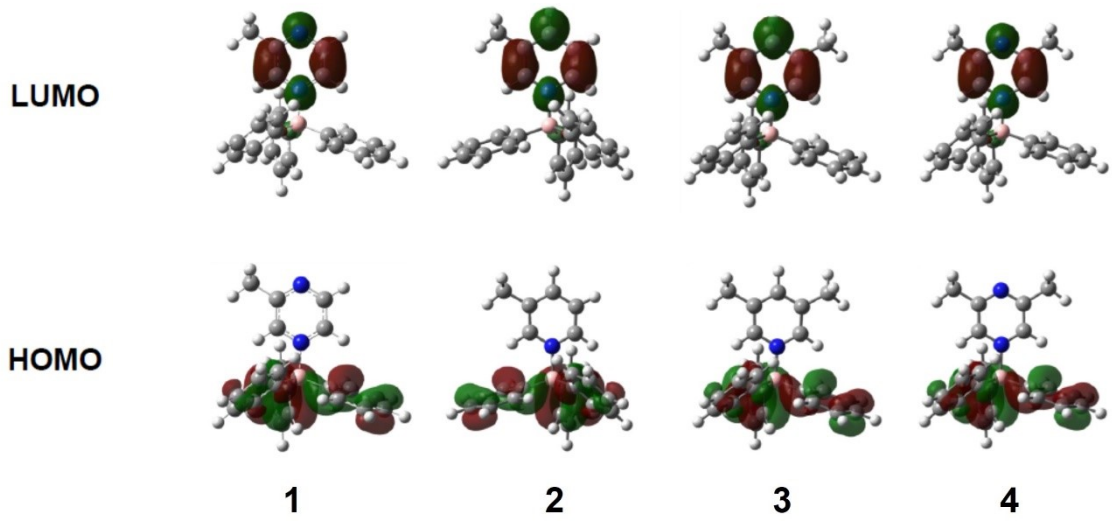

Figure S14 HOMO/LUMO plots of **1** to **4**. (B3LYP/6-31g(d) level of theory).

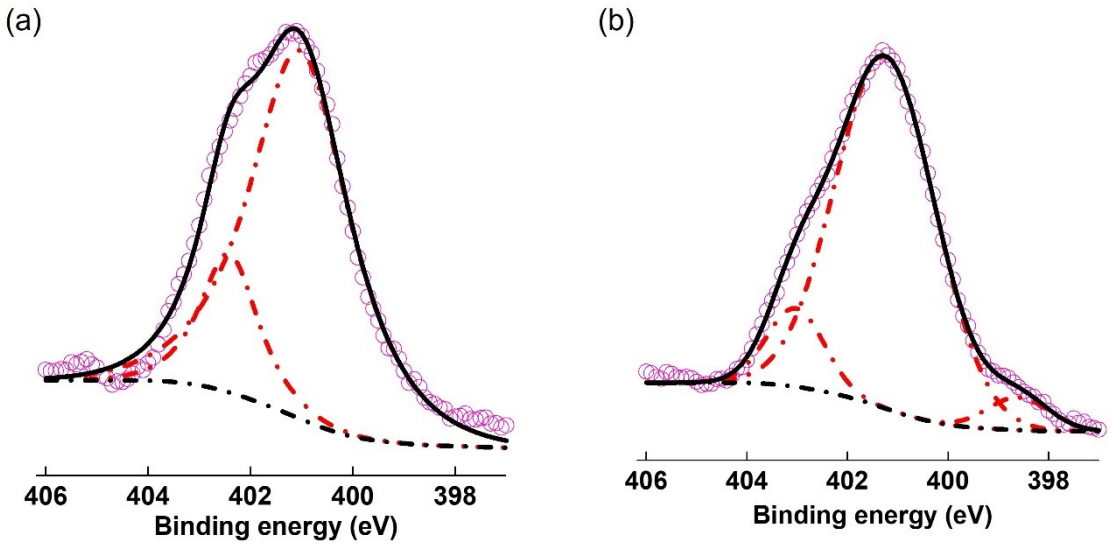

Figure S15 N 1s XPS core-level spectra of **4** before (a) and after (b) irradiation. The red dashed lines depict the resolved peaks, with the sum shown by the black solid lines. The black dashed lines indicate the baseline.

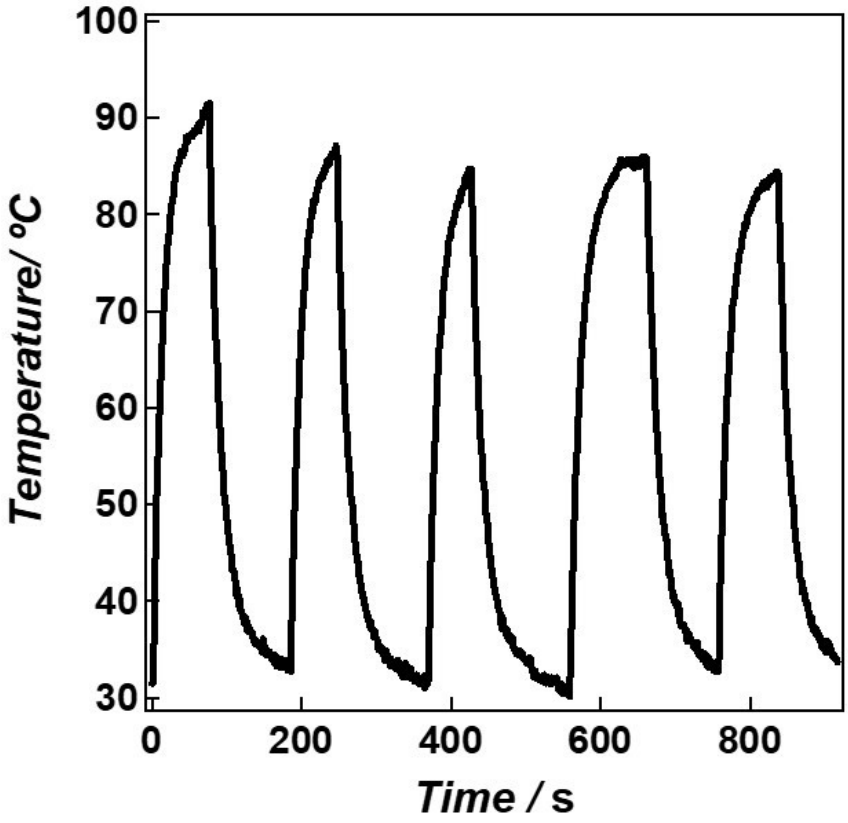

Figure S16 Photothermal cycling curve for **4_UV** (850 nm, 0.3 W/cm²).

Calculation Method for Photothermal Conversion Efficiency (*η*)

The specific heat capacities of **1** and **4** were calculated using DSC measurements and Ag_2S (around 0.7 *J*/(g·K)) as the reference material. The specific heat capacity (Cp) is defined as Cp = Q / (m × ΔT), where Q is heat (*J*) and m is mass (g). In the temperature range of 40-80 °C, the specific heat capacity of **1** is 1.12-1.26 *J*/(g-K), while that of **4** is 1.06-1.21 *J*/(g-K) (Figure S13). To calculate the thermal conversion efficiency, the average specific heat capacity from 40 to 80 °C was used.

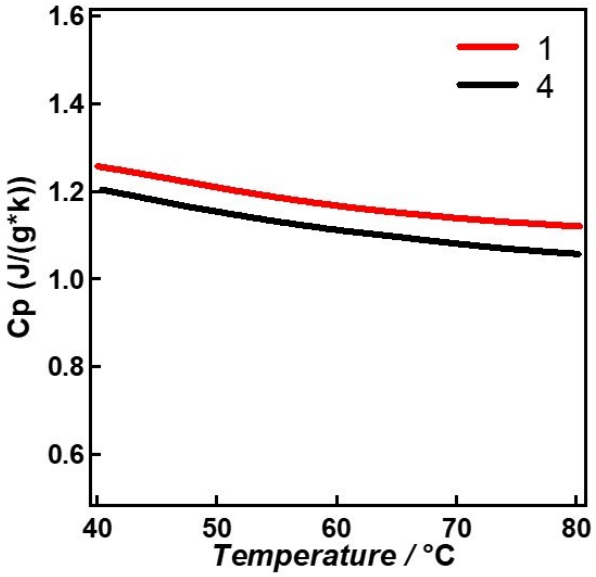

Figure S17 Specific Heat Capacity from 40 to 80 °C.

Given the information on absorbance, photothermal temperature, and heat capacity, the rough photothermal conversion efficiency (*η*) can be calculated using the method described in Ref. 23 of the main text.

$$mC_p\frac{dT}{dt} = Q_s - Q_{loss}$$

Here, *m* (using 30 mg for **1** and 50 mg for **2**) and C_p represent the mass and heat capacity of the solid, respectively, and Q_s is the photothermal energy input from irradiation, expressed by the following equation:

$$Q_s = I(1-R)_{\eta}$$

where *I* is the laser power (0.3 W/cm^{-2}), and *R* is the reflectance at the excitation wavelength of 850 nm (Figure S14). Q_{loss} is the thermal energy lost to the surroundings, which is approximately proportional to the linear thermal driving force:

$$Q_{loss} = hS(T - T_{surr})$$

where *h* is the heat transfer coefficient, *S* is the surface area of the container, and T_{surr} is the ambient temperature. When the temperature reaches its maximum, the system reaches equilibrium (Figure S14). Thus,

$$Q_s - Q_{loss} = hS(T_{max} - T_{surr})$$

(T_{max} - T_{surr}) is 54.2 K for **1**_UV and 58.9 K for **4**_UV. The conversion efficiency η is calculated as:

$$\eta = \frac{hS(T_{max} - T_{surr})}{I(1 - R)}$$

To determine *hS*, we introduce the dimensionless driving force ϑ as follows:

$$\theta = \frac{T - T_{surr}}{T_{max} - T_{surr}}$$

Derive θ with respect to *T* and we get

$$\frac{d\theta}{dt} = -\frac{Q_s}{mC_p(T_{max} - T_{surr})} - \frac{hs\theta}{mC_p}$$

When the laser is off, Q_s = 0, thus:

$$\frac{d\theta}{dt} = -\frac{hs\theta}{mC_p}$$

Integrating, we get:

$$t = -\frac{mC_p}{hs} ln\theta$$

Therefore, *hS* can be calculated from the slope of the cooling time vs. ln ϑ plot (Figure S14). *hS* is found to be 1.19919×10^{-3} J/(Ks) for **1**_UV and 2.39846×10^{-3} J/(Ks) for **4**_UV. According to the equation, the conversion efficiency η for **1**_UV and **4**_UV is finally calculated to be 66% and 82%, respectively.

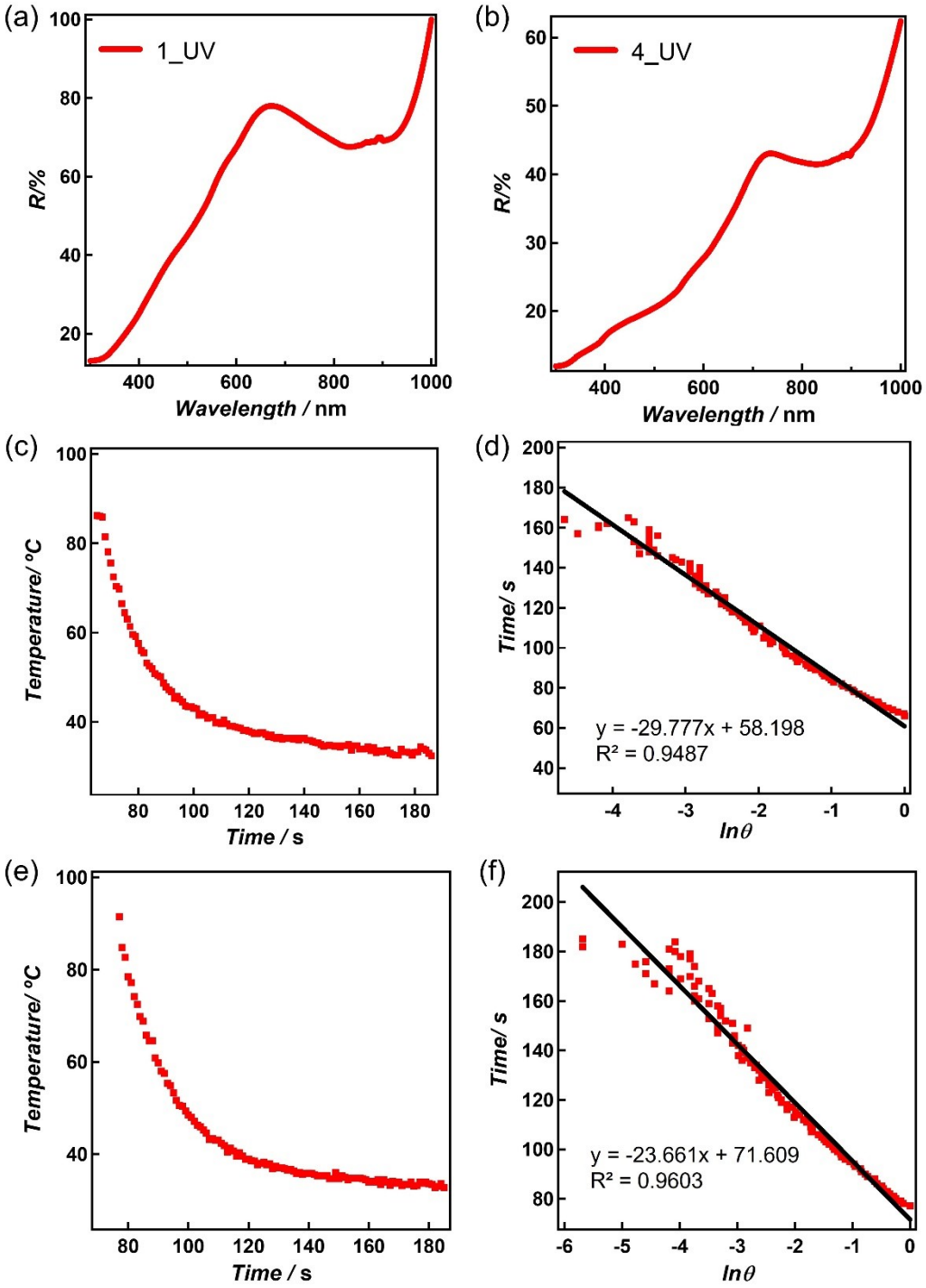

Figure S18 UV-Vis-NIR diffused reflectance spectra of **1** (a) and **4** (b) before and after UV irradiation for 10 min. The cooling curve of after irradiation of **1**_UV (c) and **4**_UV (e) with 850 nm laser (0.3 W cm^{-2}) and its corresponding time-lnϑ linear curve (d, f).